Optic models for short-pitch cholesteric and chiral smectic liquid crystals

Pascal Hubert,[1] Pontus Jägemalm,[2] Claudio Oldano,[1] and Mauro Rajteri[3]
[1]*Dipartimento di Fisica del Politecnico di Torino and Istituto Nazionale di Fisica della Materia, Corso Duca degli Abruzzi 24, 10129 Torino, Italy*
[2]*Department of Microelectronics and Nanoscience, Chalmers University of Technology, S-41296 Göteborg, Sweden*
[3]*Istituto Elettrotecnico Nazionale Galileo Ferraris, Settore Fotometria, Strada delle Cacce 91, 10135 Torino, Italy*
(Received 31 July 1997; revised manuscript received 26 January 1998)

The optical properties of cholesteric and chiral smectic-*C* liquid crystals having a pitch shorter than the light wavelength are studied, both theoretically and experimentally. A particular emphasis is placed on the optical activity. For smectics, the optical rotation is maximum for a tilt angle of 45° and for light propagating orthogonally to the helix axis; for short-pitch cholesterics, the optical activity is, in any case, very small. The limits of validity of a recently proposed macroscopic model for such media are discussed, in the framework of a more general discussion on optical models for gyrotropic media. It is shown that the macroscopic models generally work well for the bulk properties. However, for chiral smectics with the smectic planes parallel or nearly parallel to the boundary planes, no homogeneous model is able to account for the gyrotropic properties, independently of how small the pitch is and for any sample thickness. Our experimental data are in agreement with these theoretical findings. [S1063-651X(98)05509-3]

PACS number(s): 61.30.−v, 78.20.Ek, 78.20.Bh

I. INTRODUCTION

In most liquid crystal (LC) compounds the molecules are strongly elongated, and some periodic LC phases are known where the average direction $\hat{\mathbf{n}}$ (nematic director) of the long molecular axes rotates uniformly along a given direction, describing a helix. If the helix pitch is smaller than the light wavelength, the periodic medium can be conveniently treated in optics as macroscopically homogeneous, as usual for crystals. Recently, a macroscopic optical model for short-pitch chiral smectic-*C* liquid crystals (S_c^*) has been suggested [1], which also is valid for other LC phases having the same C_2 element of symmetry (S_I^*, S_F^*, and S_K^*), and includes as a particular case the cholesteric (N^*) phase. The macroscopic effective medium is uniaxial, with the optic axis along the helix axis of the periodic structure, and is optically active.

Here, a critical discussion of the model is given. It will be shown that with minor changes concerning its constitutive equations, the model can be successfully applied to the actually available short-pitch N^* and S_c^* compounds, except for some very particular optical geometries. This fact could itself motivate our investigations, owing to the increasing interest of such compounds in applications [2,3]. However, our main motivation goes beyond the optics of LCs and refers to basic optics. In fact, the search of a macroscopic model for optically active crystals is still an open problem, since this property is hardly incorporated in the framework of homogeneous models, in particular for crystals with a long range order. Here we recall some of the difficulties found in any macroscopic description of optical activity.

(1) A first difficulty comes from the fact that optical activity is only displayed by dissymmetric (chiral) objects. The models used to represent optical activity are therefore rather complicated and require heavy numerical computations. The different molecular models suggested different constitutive equations, relating the vectors **E**, **D**, **B**, and **H**, and defining the macroscopic properties of the medium. A surprisingly large number of constitutive equations are indeed found in the literature and actually used. This fact is perhaps the main source of confusion for nonspecialists (and for specialists too). For a review, see Refs. [4–6].

(2) A more substantial difficulty comes from the fact that optical activity is a nonlocal property, depending explicitly on the molecular size a. In particular, the circular birefringence of isotropic media (which is proportional to the optical rotation along a path of one wavelength) scales as a/λ, as first recognized by Boltzmann [7] on the basis of a molecular model. The optical rotation per unit length, i.e., the rotatory power, scales therefore as a/λ^2. The higher order powers of the Boltzmann ratio a/λ are generally negligible, since $a \ll \lambda$. For anisotropic media the nonlocality of the dielectric properties gives rise to spatial dispersion, namely, to the dependence of the gyrotropic parameters on both the modulus and the direction of the light wave vector. The usual frequency dispersion, which is neglected here for the sake of simplicity, gives an additional λ dependence to the simple a/λ^2 law for the rotatory power.

For gyrotropic crystals we have a further characteristic length, namely, the spatial periodicity p, and hence a contribution scaling as p/λ can appear. For the actually available chiral smectics, this contribution is dominant, since $p \gg a$, and the higher order powers of the Boltzmann ratio p/λ play a non-negligible role. For the helical-shaped LC phases an optical model is universally used where the molecular structure is neglected and the optical properties are defined by means of a local dielectric tensor $\underline{\underline{\varepsilon}}(\mathbf{r})$. Since we consider only short-pitch compounds, this model plays in our theory the role of a *mesoscopic model.*

(3) For periodic media the main difficulty comes from the fact that the eigenwaves within the medium are Bloch waves, whose Fourier components represent plane waves having

wave vectors $\mathbf{k}+\mathbf{q}$, where $\mathbf{q}$ is a vector of the reciprocal lattice. A macroscopic model is obtained by considering only the zeroth-order Fourier component and neglecting the effects of the higher order ones. Unfortunately, the amplitude of the neglected components is not negligible for actual crystals [8,9]. Despite this fact, no experimental evidence of a possible role of the neglected Fourier components has been found to date. To explain this, we recall that the higher order Fourier components give rise to a fine structure of the electromagnetic field within the crystal cells, which often has negligible influence on optical experiments, where only an average (macroscopic) field is of interest.

The above quoted problems are well known and have been discussed for a long time in the literature (see, for instance, Refs. [8,9]). We approach here the same problems on the basis of the fact that a mesoscopic and a macroscopic model for the same medium are now available, both defined by fully analytic and very simple constitutive equations. As far as we know, nothing similar can be found in the literature, at least for gyrotropic media, and all the previous discussions concerning the limits of validity of macroscopic models are based on qualitative or semiquantitative arguments. Here we give, instead, a fully quantitative analysis. Our attention will be concentrated on the possible failure of the *macroscopic homogeneous model*, considering as exact the *mesoscopic* one (periodic). As already stated, in some particular geometries strong discrepancies are indeed found. In all these cases our experiments confirm the full validity of the mesoscopic model.

II. THE MODELS

A. Mesoscopic model

In the mesoscopic model, the chiral smectic is assumed to be a continuous periodic medium that is locally uniaxial, nonmagnetic, and nongyrotropic. The optic axis is parallel to the nematic director $\hat{\mathbf{n}}$, which is uniformly rotating along z in such a way that its components are given by

$$n_x=\sin\,\alpha\,\cos(qz+\varphi_0),$$

$$n_y=\sin\,\alpha\,\sin(qz+\varphi_0), \tag{1}$$

$$n_z=\cos\,\alpha,$$

where α is the tilt angle, $q=2\pi/p$, and the phase constant φ_0 defines the direction of $\hat{\mathbf{n}}$ at the plane $z=0$, which in our experiments is considered as the first boundary of the sample. In the two limiting cases $\alpha=0$ and $\alpha=\pi/2$ we obtain a nongyrotropic homogeneous medium and a cholesteric liquid crystal, respectively.

The optical properties of the mesoscopic model are fully defined by the real dielectric tensor

$$\underline{\underline{\varepsilon}}=\varepsilon_o+\varepsilon_a\hat{\mathbf{n}}(z)\hat{\mathbf{n}}(z), \tag{2}$$

where ε_a is the local dielectric anisotropy, defined as the difference $\varepsilon_e-\varepsilon_o$ between the principal values of $\underline{\underline{\varepsilon}}$. The components of the tensor $\underline{\underline{\varepsilon}}(z)$ are periodic functions of z, with period equal to the helix pitch.

The magnetic polarizability of actually available compounds is negligibly small, whereas their local biaxiality and gyrotropy are in general non-negligible, having the same order of magnitude as for usual crystals. However, their influence on the optical properties of the smectic samples considered here is very small. The intrinsic optical activity (coming from the chirality of the individual molecules) gives non-negligible effects only in the limit where the pitch becomes comparable to the atomic size. Even in this limit, it is interesting to find out and discuss the optical activity coming from the helical arrangement of the molecules.

B. Landau-type constitutive equations for the macroscopic model

A macroscopic model for short-pitch chiral smectics has been derived in Ref. [1] in the framework of the theory of spatial dispersion, by making use of the Landau-Lifshitz formalism [10]. For harmonic plane waves the constitutive equations are written as

$$\tilde{\mathbf{D}}=\underline{\underline{\tilde{\varepsilon}}}\varepsilon_0\mathbf{E}, \tag{3a}$$

$$\mathbf{B}=\mu_0\tilde{\mathbf{H}}, \tag{3b}$$

where the vectors $\mathbf{E}$, $\tilde{\mathbf{D}}$, $\mathbf{B}$, and $\tilde{\mathbf{H}}$ are the effective values of the fields. In a perturbation expansion where only linear terms of the parameters ε_a^2 and p/λ are considered, the effective permittivity tensor is given by

$$\underline{\underline{\tilde{\varepsilon}}}=\begin{pmatrix}\tilde{\varepsilon}_o & 0 & 0\\ 0 & \tilde{\varepsilon}_o & 0\\ 0 & 0 & \tilde{\varepsilon}_e\end{pmatrix}+ig_\perp\begin{pmatrix}0 & 0 & -m_y\\ 0 & 0 & m_x\\ m_y & -m_x & 0\end{pmatrix}, \tag{4}$$

where

$$\tilde{\varepsilon}_e=\varepsilon_o+\varepsilon_a\cos^2\alpha,\quad \tilde{\varepsilon}_o=\varepsilon_o(1+\varepsilon_e/\tilde{\varepsilon}_e)/2, \tag{5}$$

$$g_\perp=-\frac{p}{\lambda}\frac{\varepsilon_a^2}{8\tilde{\varepsilon}_e}\sin^2(2\alpha), \tag{6}$$

and $\mathbf{m}=\mathbf{k}/k_0$, where $\mathbf{k}$ is the wave vector of the considered plane wave within the sample, $k_0=2\pi/\lambda$, and λ is the vacuum wavelength. The fact that $\underline{\underline{\tilde{\varepsilon}}}$ explicitly depends on $\mathbf{k}$ means that the medium displays spatial dispersion.

The effective homogeneous medium defined by Eqs. (4)–(6) is uniaxial and its optic axis is coincident with the helix axis. The real part of the permittivity tensor $\underline{\underline{\tilde{\varepsilon}}}$ displays the typical structure of uniaxial media with only two scalar parameters $\tilde{\varepsilon}_e$ and $\tilde{\varepsilon}_o$. A similar behavior is in general exhibited by the imaginary part of uniaxial gyrotropic media (and more precisely by the crystal classes C_n, D_n, with $n>2$), with two parameters $g_\parallel$ and $g_\perp$ related to the components of the vector $\mathbf{k}$ parallel and orthogonal to the optic axis, respectively. The absence of $m_z=k_z/k_0$ in Eq. (4) means that, for what concerns the considered homogeneous model, the parallel component $g_\parallel$ is equal to zero. The optical activity is thus zero for light propagating along the helix axis and reaches its maximum value for light propagating *orthogonally to the helix axis*.

The gyrotropy parameter $g_\perp$ is maximum for $\alpha=45°$, and zero for $\alpha=0°$ and $\alpha=90°$. Within the approximation of the model, the optical activity of cholesteric LCs is therefore zero, since their tilt angle is exactly 90°.

C. Post-type constitutive equations

The constitutive equations (3) are indeed very simple, but their simplicity has rather heavy counterparts. In particular, within gyrotropic media a new term must be added to $\mathbf{E}\times\mathbf{H}$ to obtain a Poynting vector $\mathbf{S}$ having the meaning of power flux density [11,12]. The continuity of the normal component of this vector at the sample boundaries implies a discontinuity of the tangential components of the field vectors $\mathbf{E}$ or $\mathbf{H}$. New boundary-type equations are therefore required to fully define the optical properties of the sample.

A discontinuity of $\mathbf{B}$ [and, from Eq. (3b), also of $\mathbf{H}$] implies the presence of a surface density current $\mathbf{j_s}$. The presence of such a current, related to a bulk magnetization $\mathbf{M}$, is strongly suggested by the fact that within any dielectric helix the polarization current gives rise to a magnetic dipole moment. The simplicity of the Landau formalism is due to the fact that the magnetization current $\mathbf{j_M}=\nabla\times\mathbf{M}$ is incorporated into the main current $\mathbf{j_P}=\partial\tilde{\mathbf{P}}/\partial\mathbf{t}$. In the bulk, this is always allowed, since Maxwell's equations remain unchanged under the transformation $\partial\tilde{\mathbf{P}}/\partial t=\partial\mathbf{P}/\partial t+\nabla\times\mathbf{M}$, if we accordingly define new vectors $\tilde{\mathbf{H}}$ and $\tilde{\mathbf{D}}$. Obviously, this transformation gives a different set of constitutive equations. One of the difficulties quoted in the Introduction is related to this fact, namely, to the difficulty in separating the effects of $\partial\mathbf{P}/\partial\mathbf{t}$ and $\nabla\times\mathbf{M}$.

A possible way to escape the above difficulty is to impose the continuity of the Poynting vector at the boundary surface. It is, however, preferable to make use of a different set of constitutive equations. In the following we make use of the equations derived by Post [13] under the requirement of relativistic covariance of all the equations used to describe the electromagnetic field, without using any microscopic models. For nonmagnetic lossless materials the Post equations can be written as

$$\mathbf{D}=\underline{\underline{\varepsilon}}\varepsilon_0\mathbf{E}+\underline{\underline{\chi}}\varepsilon_0 c\mathbf{B}, \tag{7a}$$

$$\mathbf{H}=-\underline{\underline{\chi}}^{\dagger}\varepsilon_0 c\mathbf{E}+\mu_0^{-1}\mathbf{B}. \tag{7b}$$

In the bulk, the equation systems (3) and (7) become equivalent by assuming

$$\underline{\underline{\varepsilon}}=\underline{\underline{\tilde{\varepsilon}}}+\underline{\underline{R}}^2, \tag{8a}$$

$$\underline{\underline{\chi}}=i\underline{\underline{R}}, \tag{8b}$$

where

$$\underline{\underline{R}}=\begin{pmatrix}0&0&0\\0&0&0\\0&0&g_\perp\end{pmatrix}. \tag{9}$$

For nonchiral media $\underline{\underline{\chi}}=0$ and $\underline{\underline{\tilde{\varepsilon}}}=\underline{\underline{\varepsilon}}$. The two sets of equations then become identical, and in the absence of losses, the permittivity $\underline{\underline{\varepsilon}}$ is real and symmetric. The optical activity of gyrotropic lossless media is therefore related to the pseudotensor $\underline{\underline{\chi}}$ and to the imaginary part of the tensor $\underline{\underline{\tilde{\varepsilon}}}$, which in this case is complex and Hermitian. The bulk constitutive Eq. (7), in contrast to Eqs. (3), are self-consistent with the usual assumptions of continuity for the components of the vectors $\mathbf{B}$, $\mathbf{E}$, $\mathbf{D}$, and $\mathbf{H}$ (tangential continuity for $\mathbf{E}$ and $\mathbf{H}$ and normal continuity for $\mathbf{B}$ and $\mathbf{D}$).

III. VALIDITY LIMITS OF THE MACROSCOPIC MODEL: BULK EFFECTS

To test the validity of the macroscopic model, we have considered the transmittance and the reflectance of a LC slab confined between two parallel planes, and compared the values given by the macroscopic and mesoscopic models, with particular attention to the polarization properties related to the optical activity. For the mesoscopic model, we have considered samples with the helix axis orthogonal to the boundary planes (homeotropic geometry) and samples with the helix axis parallel or obliquely oriented with respect to the boundary planes (phase grating geometry). In the first case, the periodic structure can be considered as an anisotropic stratified medium and the computations are performed by making use of the basic Berreman formalism [14]. In the other cases, an extended Berreman formalism, developed to find out the efficiencies of anisotropic gratings [15,16], has been used. For $p>\lambda$ the structure indeed acts as a phase grating, giving rise to diffracted beams. By decreasing the pitch, the diffraction angle of the higher order diffracted waves increases, and when the angle reaches 90° these waves become evanescent. For small enough p values only the zeroth-order transmitted and reflected beams survive. However, the presence of evanescent waves cannot be neglected in computations.

The most important discrepancies between the mesoscopic and macroscopic models are related to boundary type effects and will be considered in Sec. IV. In this section we consider some bulk effects, related to the fact that our macroscopic model neglects higher order terms in p/λ and ε_a.

We recall that gyrotropic crystals display pure optical rotation only for light propagating along the optic axis. In any other direction the medium transforms linear into elliptic polarization, but the presence of the gyrotropy has only small effects on most optical properties.

Let us first consider the case of a light beam parallel to the optic axis. The macroscopic model does not give optical rotation, since $g_\parallel=0$. This property is quite unexpected, since for $p>\lambda$, cholesterics and chiral smectic LCs display a huge pseudorotatory power for light propagating along to the helix axis, according to de Vries' equations [17]. A residual circular birefringence for light propagating along the helix axis survives for $p<\lambda$, but it decreases quickly by decreasing the ratio p/λ. More precisely, the rotatory power along the helix decreases two orders of magnitude if the internal wavelength changes from p (namely at the Bragg reflection band) to $2p$. For higher λ values, it decreases as λ^{-4}, and becomes negligible to any practical purpose for $\lambda>5p$. In the limit $p\ll\lambda$, the quantity $g_\parallel$ is in any case not exactly zero, but scales as $(p/\lambda)^3$.

To test the effects of $g_\perp$, we must consider light beams

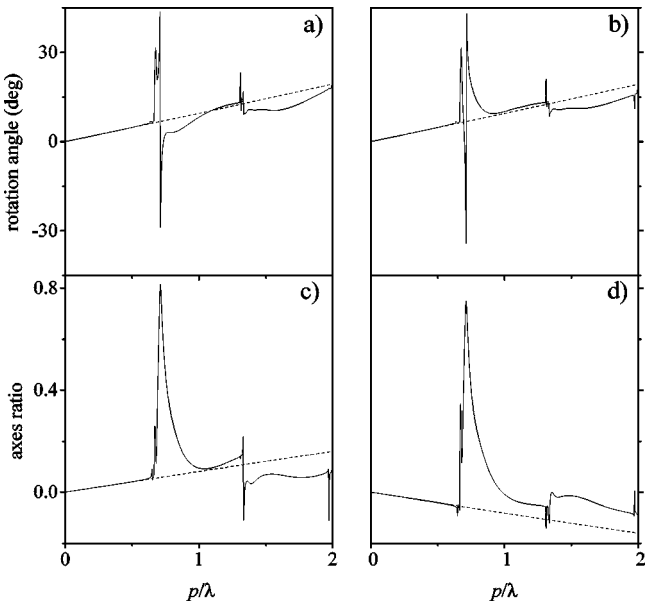

FIG. 1. Rotation angles of the major axis of the output elliptic polarization for normally incident light linearly polarized along (a) and orthogonally (b) to the helix axis, and corresponding ratios between the intensity along the minor and the major axes of the ellipse [(c) and (d)], for the helical periodic medium (solid lines) and for its macroscopic model (dotted lines). The sample is in the grating mode geometry (helix axis parallel to the boundary planes) with tilt angle $\alpha=45°$ and thickness $d=2\lambda$. Here, and in all the subsequent figures, the principal refractive indices are $n_e=1.66$ and $n_o=1.5$.

orthogonal or obliquely oriented with respect to the optic axis. These cases require a more complex analysis. We have computed the ellipticity and the directions of the ellipse axes of the transmitted and reflected beams for linear input polarization. Only for thin enough samples the polarization of the transmitted beam is nearly linear and the rotation of the major axis is simply related to $g_\perp$. It is therefore convenient to consider rather thin samples, a fact that, however, does not allow for a good separation of the bulk properties from the boundary effects.

The bulk properties are better evidenced by making use of the phase grating geometry. Therefore, we have considered this geometry to compare the optical rotations given by the macroscopic and mesoscopic models. The computations have been performed for different values of the optic parameters (p/λ, ε_a, tilt angle, input polarization, and incidence angle). The results can be summarized as follows.

For the bulk properties, the macroscopic model works well for any realistic value of ε_a, despite the fact that only terms up to ε_a^2 have been considered. For what concerns the pitch, the range of validity of the macroscopic model in the grating mode geometry is unexpectedly large, going up to the p value corresponding to the first Bragg peak, as shown in Fig. 1. It is obvious that in the Bragg regime, where the Bloch waves of the periodic medium represent standing waves, the macroscopic (homogeneous) models lose any meaning. Near the Bragg bands the Boltzmann scaling law is no longer valid and the role of the higher order terms in the power series expansion of the function $\varepsilon(p/\lambda)$ becomes important (similar behavior is found in crystals displaying circular dichroism around an absorption line). At lower p values, our computations suggest that the first neglected term in the expression of $g_\perp$ is the one scaling as $(p/\lambda)^3$, which gives again negligible effects for $p<\lambda/5$.

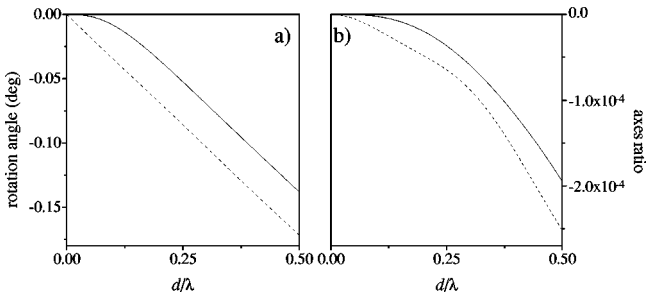

FIG. 2. Rotation angles (a) and axes ratios (b) for the same optical geometry of Fig. 1, as a function of the normalized sample thickness, for the periodic medium (solid line) and its homogeneous model (dotted line), for $\alpha=30°$, $p=\lambda/3$, and TM input polarization.

IV. VALIDITY LIMITS OF THE MACROSCOPIC MODEL: BOUNDARY EFFECTS

In the following we will consider two types of boundary effects, having different origins.

(a) Matter is intrinsically discontinuous and a sample has never a defined ''boundary surface.'' This is a trivial observation, but must not be neglected at least for what concerns a nonlocal property as optical activity. In our macroscopic description it is convenient to define a thin boundary ''transition layer'' where the optical properties are changing gradually.

(b) The macroscopic models for periodic media neglect the higher order Fourier components of the Bloch waves, whose effects are in principle very long ranged and cannot be accounted for by simply considering a thin transition layer at the boundaries (moreover, it is not self-evident that a description in terms of bulk properties and boundary conditions is allowed for crystals).

In the framework of our theory a quantitative account of both these effects can be done. The computations have been performed for different values of the parameters of interest: incident angle, sample thickness, pitch, and wavelength. We have found that effects of type (b) are indeed present if the boundary layers are orthogonal or nearly orthogonal to the helix axis, i.e., in the homeotropic or nearly homeotropic geometry.

A. Phase grating geometry and transition layer

The presence of boundary transition layers is well evidenced by Fig. 2(a), which refers to a sample with the helix axis parallel to the boundary planes. The homogeneous model gives an optical rotation that increases linearly with the sample thickness. The mesoscopic model, instead, gives practically no rotation if the sample thickness is small with respect to the helix pitch. To account for this effect in the framework of a macroscopic description, we must assume that $g_\perp$ is gradually changing from zero (at the sample boundary) to the bulk value. Nothing similar has been found

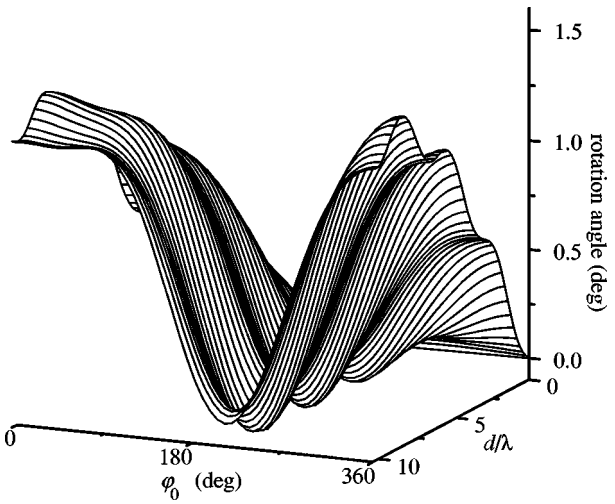

FIG. 3. Rotation angle in the homeotropic geometry as a function of the normalized sample thickness and of the phase constant φ_0 (which defines the direction of the local optic axis at the input plane), for $p=\lambda/3$, $\alpha=30°$, and incidence angle of 40°.

for the parameters $\tilde{\underline{\underline{\varepsilon}}}_e$ and $\tilde{\underline{\underline{\varepsilon}}}_o$. For thin samples, large discrepancies between the mesoscopic and the macroscopic models are only found for the optical properties related to the parameter $g_\perp$, as, for instance, the output ellipticity for input TM polarization [Fig. 2(b)].

This fact has interesting consequences for what concerns the thin film interference patterns. We expect that the presence of the transition layers at the sample boundaries will lower the amplitudes of the interference fringes. In fact, in the phase grating mode geometry the interference patterns computed on the basis of the exact mesoscopic model are generally attenuated and disappear completely in some optical conditions [18]. We have not been able to experimentally test these effects because the surface interactions cause the helix to unwind in thin cells and because our samples are in any case not perfectly monodomain.

B. Homeotropic geometry and breaking down of homogeneous model

The phases of the Fourier components of the Bloch waves are at any point related to the phase $\varphi=\varphi_0+qz$ of the periodic helical structure of the medium at the same point. The phase constant φ_0 plays therefore the role of a control parameter for these phases. In the homeotropic geometry the phase φ is constant at each boundary plane and a change of the phase φ_0 has the same effect as a rotation of the whole sample with respect to the incidence plane of the light. We therefore expect a dependence of the optical properties of the actual periodic medium on φ_0, whereas the properties of the homogeneous model are independent of the parameter φ_0, which does not appear in its constitutive equations (3)–(9).

The dependence of the rotation angle on φ_0 given by the mesoscopic model is shown in Fig. 3 for an incidence angle of 40°. This dependence is very strong for any incidence angle. Surprisingly, *it does not decrease by increasing the thickness of the sample*, as shown in Fig. 4. This dependence must therefore be considered as a true breaking down of the homogeneous model, not as a simple boundary effect. It is a

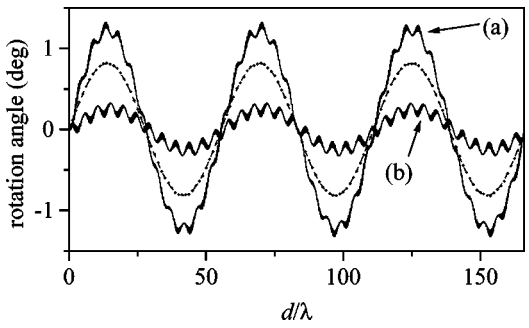

FIG. 4. Rotation angle as a function of the normalized sample thickness for $\varphi_0=0°$ (a) and $\varphi_0=220°$ (b), with the same parameters as in Fig. 3. The points and the dotted line, which are nearly coincident, give the rotation averaged over φ_0 and the rotation computed according to the macroscopic model, respectively. [Curves (a) and (b) present a fine structure, not fully resolved, of interference fringes.]

''boundary'' only in the sense that φ_0 defines the direction of the local optic axis at the boundary plane $z=0$ (and at the second boundary plane if the sample contains an integer number of pitches). By decreasing the ratio p/λ we obtain curves practically identical to the ones plotted in Figs. 3 and 4, but with smaller rotation angles. The optical rotation and its derivative with respect to φ_0 scale as p/λ, according to the Boltzmann law.

Discrepancies between the mesoscopic and macroscopic models are also found in the reflectance curves from a semi-infinite sample. For a TM (or TE) polarized incident beam, the homogeneous model gives a TM (or TE) polarized reflected beam since the macroscopic optic axis lies in the incidence plane. The mesoscopic model, instead, gives in general an elliptic polarization, since the local optic axes near the boundary planes do not lie in the incidence plane. The dependence of the reflectance on φ_0 appears here as obvious if we consider that a change of φ_0 is equivalent to a rotation of the local optic axes at the boundary planes. Interestingly, a φ_0 change has strong effects on the optical properties related to optical activity, whereas it has generally small effects for the other optical properties. In fact, the total intensity of the reflected beam is practically independent of φ_0, as shown by Fig. 5(a), where the curves computed with different values of φ_0 are practically coincident. On the contrary, the polarization properties depend strongly on φ_0, as shown by the curves plotted in Figs. 5(b) and 5(c), which again scale as p/λ. Figure 5(d) shows a new φ_0-dependent boundary effect, consisting of a small dephasing between reflected and incident beams (we recall that the dephasing for homogeneous lossless media is equal to zero or to 180°).

The failure of the homogeneous model can also be understood on the basis of the following argument: consider a sample in the phase grating oblique geometry. The grating constant (i.e., the spatial period of the grating) is equal to $p/\sin\delta$, where δ is the angle between the helix axis and the boundary normal. For small enough δ values, the grating gives a set of diffracted beams (which do not satisfy the Bragg law since the grating works in the Raman-Nath regime). Obviously, no homogeneous model can be used to approximate a grating.

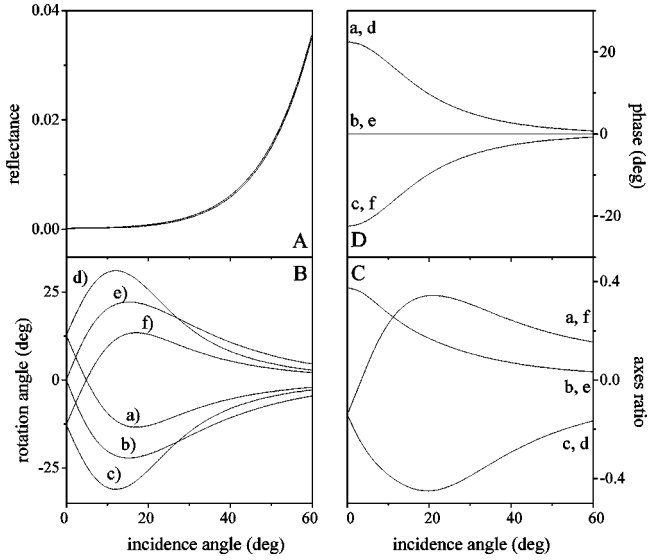

FIG. 5. Polarization parameters (intensity, phase, rotation of the main ellipse axis, and axes ratio) of the beam reflected by a semi-infinite sample with the helix axis orthogonal to the boundary planes, as a function of the incident angle for input TM polarization and for different values of φ_0: (a) 30°, (b) 90°, (c) 150°, (d) 210°, (e) 270°, and (f) 330° ($p=\lambda/4$, $\alpha=45°$, and $d=\lambda$).

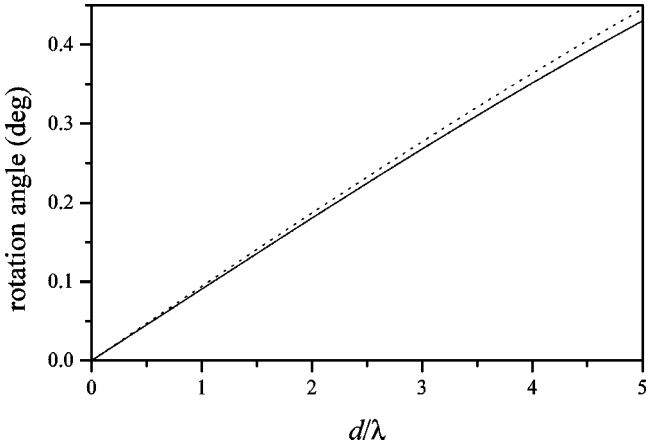

FIG. 6. Rotation angles as a function of the normalized sample thickness averaged over φ_0 (full line) for the same optical geometry and the same parameters as in Fig. 3, and the corresponding angles given by the homogeneous model (dotted line).

A failure of the homogeneous model is expected for any periodic structure as, for instance, for three-dimensional crystals. The fact that no homogeneous model is able to fully account for the optical properties of crystals is in a sense obvious. Here, we focus the conditions in which the homogeneous models fail.

It is, however, to be observed that the failure of the macroscopic model involves rather small effects and is particularly evident only in the cases where both optical activity (i.e., a nonlocal property) and the higher order Fourier components play an important role. Further, we expect that an averaging of the reflectance and transmittance over φ_0, which is equivalent to average over the phase constants of the neglected Fourier components, could restore the validity of the homogeneous model. The *averaged curves* are in fact rather well fitted by our homogeneous model, as shown by Figs. 4 and 6 (indeed, in Ref. [1] the homogeneous model has been defined by averaging over φ_0 the transfer matrix of planar samples, i.e., the matrix relating the field vectors **E** and **H** at the sample boundaries). This fact is of the most importance from the experimental point of view. Many sources of averaging are always present in actual experiments (as, for instance, nonperfect flatness of glasses, inhomogeneous anchoring of the smectic structure, and more generally nonperfect periodicity due to various defects), which are expected to become more efficient by decreasing the pitch of the helical structure or the spatial period of other periodic media. So, we draw the conclusion that homogeneous models for crystals could work well in actual experiments, and even in optical geometries where they are conceptually wrong. The main aim of our experiments is to test this important point.

Finally, we notice that the boundary effect related to the presence of a transition layer does not appear in the homeotropic geometry (Fig. 6). This can have important implications for nonperfect crystals if the long range helical order is lost (owing to some source of randomness), with different correlation lengths in different directions. By comparing Figs. 2(a) and 6, we expect that the optical activity is practically unchanged if the order is lost along the helix direction, whereas it decreases if the order is lost in the orthogonal direction.

V. EXPERIMENTS

The experiments were performed with the ZKS-2502 compound. This compound is in the chiral smectic-*C* phase at room temperature, with a pitch of about 0.17 μm, tilt angle $\alpha=26°$, and effective optical anisotropy $\Delta\tilde{n}=0.16$. The cells were prepared by enclosing the liquid crystal between two identically treated glass plates, which were separated with either evaporated SiO films or Mylar spacers. Samples of different thickness were prepared ($d=4$, 2, and 1.6 μm) in both the homeotropic and the phase grating geometries, i.e., with the helix axis perpendicular or parallel to the boundary planes, respectively. The homeotropic orientation was obtained by depositing a lecithin layer on the glass plates. To obtain the phase grating orientation, a unidirectional mechanical shear of the cell substrates was applied. A polarization microscope was used to control the quality of the samples and the direction of the helix axis. For the homeotropic geometry, the helix axis is orthogonal to the boundaries only where the sample appears as uniformly black between crossed polarizers. A more complex analysis is required to find out the direction of the helix axis, i.e., the macroscopic optic axis, in the phase grating geometry. We have first looked for the direction of the input polarization where the transmittance of the sample between crossed polarizers reaches a minimum. The parallelism between the optic axis and the boundary planes was then ensured by considering the symmetry of the transmittance curves under a sign change of the incidence angle. The measurements were performed with a 10 mW He-Ne laser ($\lambda=0.6328$ μm), which was linearly polarized with a prism polarizer. The

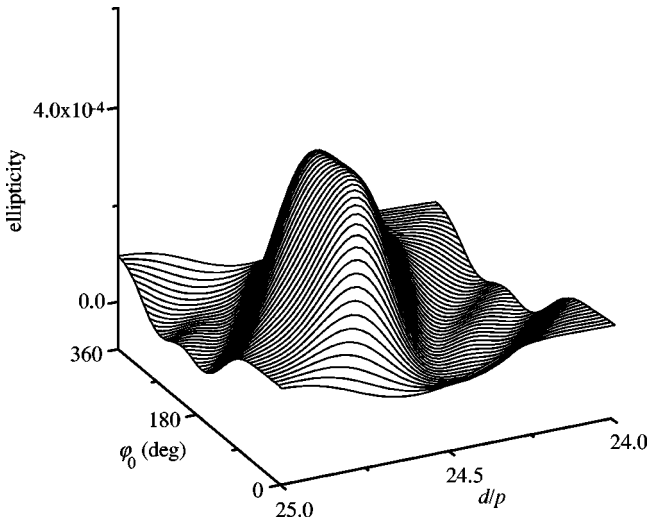

FIG. 7. 3D representation of the ellipticity (squared ratio of the ellipse axes) as a function of the phase constant φ_0 and of the normalized thickness. The parameters are the same as in Fig. 5.

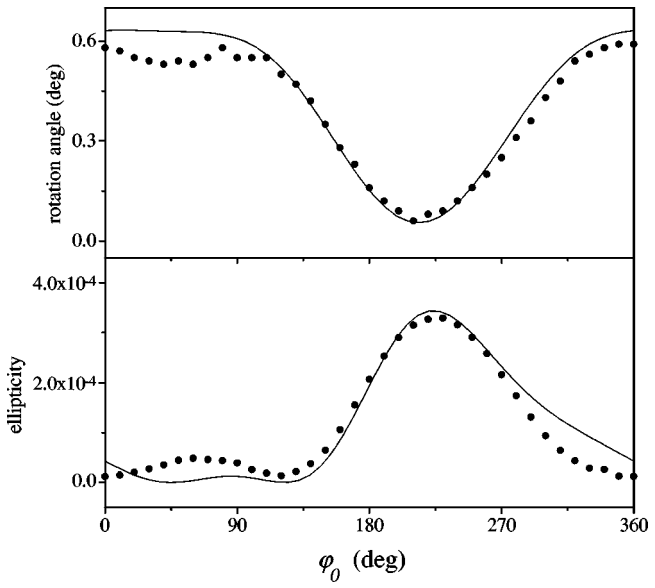

FIG. 8. Polarization parameters (ellipticity and rotation angle) of the transmitted beam as a function of the orientation φ_0 of a homeotropic sample, for incident TM polarization: experimental data (circles) and theoretical fit (solid lines) for nominal values of the material parameters and with a best fit thickness of 4.14 μm.

outcoming light from the sample was analyzed with a Glan-Thomson polarizer, which could be rotated by a step motor with a resolution of 0.05°. The light was detected with a silicon photodiode whose output signal was sent to a variable gain amplifier. The position of minimum and maximum intensities, obtained by rotating the analyzer, correspond to the directions of the minor and major axis of the output polarization ellipse, respectively, and the intensity ratio gives the square of the axes ratio. The angle between the main axis of the ellipse and the polarization direction of the incident light is considered as the rotation angle.

Curves giving the square of the axes ratio (ellipticity) and the rotation angle as a function of the incident angle and the input polarization direction were obtained and compared to the theoretical curves given by the mesoscopic model (exact). A best fit procedure of these measurements is not only a test of the validity of the model, but also a way to obtain all the optical parameters of the liquid crystal cell (thickness, pitch, tilt angle, birefringence, and phase constant φ_0). In fact, our computations reveal that the output ellipticity shows a strong dependence on all these parameters. An evidence of this property is shown in Fig. 7, which is a three-dimensional plot of the ellipticity as a function of the phase constant φ_0 and of the normalized thickness d/p for light at normal incidence on a perfect homeotropic sample. In this case, a change in φ_0 can be obtained by rotating the input polarization or the sample around its normal, equivalently. However, further experiments and an improvement of the preparation procedure of the samples are required for a precise determination of the material parameters. Our homeotropic samples are instead good enough to evidence the important effect discussed in Sec. IV B, i.e., the fact that a simple rotation of the sample around its macroscopic optic axis drastically changes the transmittance. This is shown in Fig. 8, which refers to a sample with nominal thickness $d=4$ μm. The experimental points obtained by a sample rotation (circles) are rather well fitted by the theoretical curves computed on the basis of the mesoscopic model, by assuming a perfectly monodomain sample with $d=4.14$ μm and nominal values of the other parameters (solid lines). The estimated experimental errors (mainly related to the sample defects) are of the same order of magnitude as the differences between theoretical and experimental curves. We have therefore at the same time proved the rather good quality of the sample preparation procedure (remember that any source of defects always gives some type of averaging over φ_0), the validity of the mesoscopic model and the failure of the macroscopic models.

VI. CONCLUSIONS

A great emphasis has been given in the literature to the optical properties of cholesteric and chiral smectic liquid crystals for light propagating along the helix axis, since those properties are at the same time very interesting and can be expressed by simple analytic expressions [17]. The optical properties of the now available short-pitch cholesteric and chiral smectics are even simpler for any direction of the light beam, since the periodic helical structure can be considered as a homogeneous uniaxial medium (here referred to as the macroscopic model), whose optical properties can be described by the same constitutive equations valid for usual crystals [1]. Two different and equivalent sets of constitutive equations have been considered, making use of the Landau and Post formalism. In the first set, the bulk properties are described by a complex tensor $\tilde{\tilde{\varepsilon}}$ and the tangential components of $\tilde{\mathbf{H}}$ are discontinuous. So we have preferred to make use of the Post equations, where the bulk properties are described by two real tensors $\underline{\underline{\varepsilon}}$ and $\underline{\underline{\chi}}$, and the boundary conditions are expressed by the usual requirement of continuity for the tangential components of the vectors **E** and **H** and for the normal components of the vectors **B** and **D**. In both sets

only three scalar parameters appear, which are simply related to the parameters defining the periodic structure (referred to as the mesoscopic model, which in our theory plays the role of the microscopic models for usual crystals). In general, the symmetry class requires four parameters, which are the two dielectric constants $\tilde{\varepsilon}_e = \tilde{\varepsilon}_\perp$ and $\tilde{\varepsilon}_o = \tilde{\varepsilon}_\parallel$ appearing in $\underline{\underline{\varepsilon}}$, and the two corresponding gyrotropic parameters $g_\parallel$ and $g_\perp$ appearing in $\underline{\underline{\chi}}$. In our case, $g_\parallel$ is equal to zero. This means that the well known pseudorotatory power of cholesteric and chiral smectic-*C* liquid crystals for light propagating along the helix axis goes to zero in the limit of short pitches. The optical rotation is only given by $g_\perp$, and is therefore maximum for light propagating orthogonally to the helix axis. The dependence of $g_\perp$ on the pitch p and on the tilt angle α is such that the rotation rate scales as p/λ^2 and is proportional to $\sin^2(2\alpha)$. The optical activity is thus practically absent in short-pitch cholesterics, where $\alpha = 90°$.

The central point of our research is the discussion of the limits of validity of macroscopic models, by considering as exact the mesoscopic one. The main interest of the research is connected to the difficulty in inserting optical activity in any macroscopic description of matter. In fact the optical activity is one of the optical effects (the most important one) arising from the molecular structure of matter, and is therefore hardly accommodated in the framework of a ''continuum'' theory, which neglects the molecular structure. We have shown that this difficulty is something more than a hypothetical paradox and focused on the point where the macroscopic description can fail. We recall here the most important points.

The macroscopic model has been derived by considering the limit $p \ll \lambda$, but for the nongyrotropic properties it works well in any optical geometry up to $p \approx \lambda/5$. Instead, it fails seriously for the gyrotropic properties of chiral smectics in the homeotropic geometry, *for any value of the pitch and for any thickness of the sample*. According to any homogeneous model, a rotation of the sample around the macroscopic optic axis (which is orthogonal to the boundary planes) has no effect on the transmittance and reflectance. On the contrary, a rotation of the actual periodic sample changes the amplitudes of the transmitted and reflected beams and could even change the sign of the optical rotation (this important fact has been proved both theoretically and experimentally). This means that no homogeneous model is able to describe the optical activity of the periodic medium. It is already known [19] that different macroscopic models for gyrotropic media can give different reflection coefficients, a fact that reflects the difficulty of finding out the correct boundary conditions for such models. According to our computations, the discrepancies among the different models are generally small as compared to the discrepancies between any one of the models and the actual periodic medium.

Interestingly, by averaging the amplitudes of the transmitted and reflected waves given by the mesoscopic model over the rotation angle φ_0, we obtain practically the same amplitudes as those given by the macroscopic model. The failure of the macroscopic model is due to the fact that it neglects the higher order Fourier components, since the rotation shifts the phases of all these components. An averaging over the rotation angle is therefore equivalent to an averaging over the phases of the neglected components, a procedure that restores the validity of the macroscopic model. It is important to observe that other sources of phase averaging are always present in actual (nonperfect) crystals, which again could restore the validity of the macroscopic model. On the basis of the above discussion we can presume that the macroscopic models universally used in optics for usual crystals could similarly fail if the crystal boundaries are coincident with the lattice planes and the surfaces are perfectly flat without too many defects.

We conclude with some further comments. A few years after the discovery of optical activity, Fresnel was able to explain the effect by simply assuming circular birefringence, i.e., different refractive indices for left and right circular polarizations. By analogy with the helical morphology of circularly polarized waves, he suggested a helixlike structure for optically active media [20]. The advent of x-ray diffraction techniques offered the possibility to experimentally test Fresnel's hypothesis for usual crystals. A different way to test the same hypothesis is given by cholesteric liquid crystals, whose morphology is exactly the same as the one of circularly polarized light. As well known, a cholesteric sample is indeed able to rotate the polarization plane of light, but this effect is not the same as for usual optically active media [21,22]. Further, the rotation becomes practically zero if we extrapolate the cholesteric pitch to molecular dimensions. Only in the last years it has been shown that the helical smecticlike phases display true rotatory power. Fresnel's hypothesis is now confirmed, but certainly not in the sense he expected, since the helical structure gives optical rotation for light propagating orthogonally to the helix. Once again, the study of liquid crystals greatly helps our understanding of basic physics.

We have considered chiral smectic-*C* liquid crystals, which represent the first example of media whose optical rotation is described by simple analytic expressions. We expect that similar expressions will be found for other media, and in particular (1) for smecticlike structures, similar to the cholestericlike structures, recently studied by Lakhtakia and co-workers [23,24]; (2) for helixlike structures appearing in nematics undergoing a Meyer [25] or Pikin [26] type Fréedericksz phase transition, where the direction of the helix axis and the grating wave vector are orthogonal (whereas in S_c^* they are parallel); (3) for the recently discovered twist grain boundary (TGB) phases [27,28], which display discrete rotation of the optic axis along a given direction; (4) for two- and three-dimensional helixlike structures, as, for instance, the ones appearing in the Blue [29] and in the TGBC* [27] phases. The existence of a second helical ordering in these two last structures gives rise therefore to an intermediate complexity between the one-dimensional and the three-dimensional periodicity, allowing for a further step towards the optics of usual crystals.

[1] C. Oldano and M. Rajteri, Phys. Rev. B **54**, 10 273 (1996).
[2] J. Fünfschilling and M. Schadt, Jpn. J. Appl. Phys., Part 1 **35**, 5765 (1996).
[3] P. Rudquist, L. Komitov, and S. T. Lagerwall, Phys. Rev. E **50**, 4735 (1994).
[4] E. U. Condon, Mod. Phys. **9**, 432 (1937).
[5] A. Lakhtakia, *Selected Papers on Natural Optical Activity*, SPIE Milestones Series Vol. MS15 (SPIE, Bellingham, WA, 1991).
[6] A. Lakhtakia, *Beltrami Fields in Chiral Media* (World Scientific, Singapore, 1994).
[7] For a brief review and references, see S. F. Mason, *Molecular Optical Activity and the Chiral Discriminations* (Cambridge University Press, Cambridge, 1982), p. 18.
[8] V. M. Agranovich and V. L. Ginsburg, *Spatial Dispersion in Crystal Optics and the Theory of Excitons* (Wiley, London, 1964).
[9] V. M. Agranovich and V. L. Ginsburg, *Crystal Optics with Spatial Dispersion and Excitons* (Springer-Verlag, Berlin, 1984).
[10] L. Landau and M. Lifshitz, *Electrodynamics of Continuous Media* (Pergamon, London, 1960).
[11] H. Chipart, Compt. Rend. **178**, 1967 (1924).
[12] F. J. Fedorov, Opt. Spectrosc. **6**, 49 (1959).
[13] E. J. Post, *Formal Structure of Electromagnetics* (North-Holland, Amsterdam, 1962).
[14] D. W. Berreman, J. Opt. Soc. Am. **62**, 502 (1972).
[15] K. Rokushima and J. Yamakita, J. Opt. Soc. Am. **73**, 901 (1983).
[16] P. Galatola, C. Oldano, and P. B. Sunil Kumar, J. Opt. Soc. Am. A **11**, 1332 (1994).
[17] H. de Vries, Acta Crystallogr. **4**, 219 (1951).
[18] M. Becchi and P. Galatola (unpublished).
[19] M. P. Siverman, Lett. Nuovo Cimento **43**, 378 (1985); J. Opt. Soc. Am. A **3**, 830 (1986).
[20] S. F. Mason, *Molecular Optical Activity and the Chiral Discriminations* (Ref. [7]), pp. 3–6.
[21] N. Isaert, J. P. Berthault, and J. Billiard, J. Opt. **11**, 17 (1980).
[22] P. G. de Gennes and J. Prost, *The Physics of Liquid Crystals* (Clarendon Press, Oxford, 1993).
[23] A. Lakhtakia and W. S. Weiglhofen, Proc. R. Soc. London, Ser. A **448**, 419 (1995).
[24] K. Robble, M. J. Brett, and A. Lakhtakia, Nature (London) **384**, 616 (1996).
[25] F. Lonberg and R. B. Meyer, Phys. Rev. Lett. **55**, 718 (1985).
[26] S. A. Pikin, *Structural Transformations in Liquid Crystals* (Gordon and Breach, New York, 1991).
[27] S. R. Renn and T. C. Lubensky, Phys. Rev. A **38**, 2132 (1988).
[28] L. Navailles, P. Barois, and H. T. Nguyen, Phys. Rev. Lett. **71**, 545 (1993).
[29] V. A. Belyakov and V. E. Dmitrienko, Sov. Phys. Usp. **28**, 535 (1986).